

# Synergy of Theory and Experiment in the Remote Functionalization of Aliphatic Nitriles by “Bare” Fe(I) and Co(I) Cations in the Gas Phase<sup>†</sup>

Max C. Holthausen,<sup>‡</sup> Georg Hornung, Detlef Schröder, Semiha Sen, Wolfram Koch,\* and Helmut Schwarz\*

*Institut für Organische Chemie der Technischen Universität Berlin, Strasse des 17 Juni 135, D-10623 Berlin, Germany*

*Received March 21, 1997<sup>⊗</sup>*

The remote functionalization of aliphatic nitriles by the “bare” transition-metal ions Fe<sup>+</sup> and Co<sup>+</sup> has been investigated by means of extensive quantum chemical calculations and tandem mass spectrometry. The present investigation focuses on the chemo- and regioselectivity of bond activation, using an adequate computational strategy in conjunction with extensive labeling experiments. Nonanitrile, decanitrile, and undecanitrile have been studied experimentally; both metal ions exhibit an overall similar reactivity pattern, and molecular hydrogen, methane, and small olefins, respectively, are formed as major neutral fragments. In the theoretical study, structural and energetic aspects of the nonanitrile/M<sup>+</sup> complexes have been investigated in great detail. For both Fe<sup>+</sup> and Co<sup>+</sup>, the most favorable pathway of bond activation proceeds via initial C–H bond insertion at C(8), followed by exocyclic activation of a C–H bond and reductive elimination of molecular hydrogen via a multicentered transition structure. The calculated barriers lead to predictions with regard to the chemo- and regioselectivity of C–H and C–C bond activation pathways, and these predictions nicely agree with the findings of experiments performed afterward. In contrast to earlier experimental results, the present calculations reveal no evidence for the two metal ions Fe<sup>+</sup> and Co<sup>+</sup> to activate CH-bonds at different positions in the aliphatic chain. The implications of the present investigations are used to derive a more general mechanistic picture of remote functionalization in the gas phase.

## Introduction

The chemical inertness of saturated hydrocarbons is a consequence not only of their small polarizabilities but also of the high C–H and C–C bond strength together with the lack of energetically low-lying unoccupied orbitals. Although the chemical transformation of non-activated C–H and C–C bonds is difficult to achieve, it is not impossible, and for this purpose a variety of reagents have been developed which often contain transition metals.<sup>1</sup> However, a general problem concerns the lack of selectivity, because a reagent capable of activating alkanes is also likely to activate almost any chemical bond in functionalized organic molecules; in addition, high reactivity of a reagent is often accompanied by a decrease in selectivity. In order to resolve this dilemma, a deeper understanding of reaction mechanisms at a molecular level is mandatory, thus permitting the development of tailor-made reagents capable of selective functionalizations of C–H and/or C–C bonds.

One of the simplest experimental approaches to study fundamental principles of bond activation by transition

metals is provided by gas-phase studies in which the reactivity of “naked” or partially ligated transition-metal ions<sup>2</sup> can be assessed under well-defined conditions, without being clouded by the cooperative influences of counterions, solvents, aggregation, etc.<sup>3</sup> In the course of these promising studies, by serendipity a hallmark was discovered in the reactions of monofunctionalized alkanes with bare transition-metal cations, and this is the regioselective activation of C–H and C–C bonds well separated from the functional group.<sup>4</sup> Following Breslow’s seminal studies on biomimetic synthesis,<sup>5</sup> these processes have been referred to as *remote functionalization* in the gas phase. In remote functionalization, a bare or ligated transition-metal cation is first complexed to the functional group and then directed toward a certain region of the aliphatic backbone of the substrate.<sup>4,6</sup> The regioselectivity depends on the transi-

(2) Selected reviews: (a) Eller, K.; Schwarz, H. *Chem. Rev.* **1991**, *91*, 1121. (b) Eller, K. *Coord. Chem. Rev.* **1993**, *126*, 93. (c) Freiser, B. *S. Acc. Chem. Res.* **1994**, *27*, 353.

(3) Schröder, D.; Heinemann, C.; Koch, W.; Schwarz, H. *Pure Appl. Chem.* **1997**, *69*, 273.

(4) Reviews: (a) Schwarz, H. *Acc. Chem. Res.* **1989**, *22*, 282. (b) Czekay, G.; Drewello, T.; Eller, K.; Lebrilla, C. B.; Prüsse, T.; Schulze, C.; Steinrück, N.; Sülzle, D.; Weiske, T.; Schwarz, H. In *Organometallics in Organic Synthesis*; Werner, H., Erker, G., Eds., Springer: Heidelberg, 1989; Vol. 2, p 203.

(5) (a) Breslow, R. *Chem. Soc. Rev.* **1972**, *1*, 553. (b) Breslow, R. *Acc. Chem. Res.* **1980**, *13*, 170. (c) Breslow, R. *Acc. Chem. Res.* **1995**, *28*, 146.

(6) (a) Tsarbopoulos, A.; Allison, J. *J. Am. Chem. Soc.* **1985**, *107*, 5085. (b) Stepnowski, R. M.; Allison, J. *Organometallics* **1988**, *7*, 2097. (c) Prüsse, T.; Drewello, T.; Lebrilla, C. B.; Schwarz, H. *J. Am. Chem. Soc.* **1989**, *111*, 2857. (d) Hankinson, D. J.; Miller, C. B.; Allison, J. *J. Phys. Chem.* **1989**, *93*, 3624.

<sup>†</sup> Dedicated to Dieter Seebach, Zürich, on the occasion of his 60th birthday.

<sup>‡</sup> Present address: Cherry L. Emerson Center for Scientific Computation and Department of Chemistry, Emory University, 1515 Pierce Drive, Atlanta, GA 30322.

<sup>⊗</sup> Abstract published in *Advance ACS Abstracts*, June 1, 1997.

(1) (a) Hill, C. L. *Activation and Functionalization of Alkanes*; Wiley: New York, 1989. (b) Davies, J. A., Watson, P. L., Liebman, J. F., Greenberg, A., Eds. *Selective Hydrocarbon Activation*; VCH: Weinheim, Germany, 1990.

tion metal,<sup>4,7</sup> additional ligands,<sup>8</sup> the functional group,<sup>4</sup> and the conformational flexibility of the aliphatic chain as well as the presence of stereogenic centers in the backbone.<sup>9</sup>

In the present study, we will focus on the mechanistic aspects of the remote functionalization of medium-sized, linear aliphatic nitriles (C<sub>9</sub>–C<sub>11</sub>) by the late-transition-metal cations Fe<sup>+</sup> and Co<sup>+</sup>. As reported earlier, the metastable ion (MI) complexes undergo unimolecular losses of molecular hydrogen, olefins, and alkanes, respectively. Based on previous studies, the generalized reaction mechanism involves the following steps:<sup>4</sup> (i) initial coordination (“docking”) of the transition-metal ion M<sup>+</sup> to the cyano group of the nitrile, (ii) recoil of the aliphatic chain such that remote C–H/C–C bonds become accessible for M<sup>+</sup>, (iii) C–H or C–C bond activation via oxidative addition to yield the corresponding insertion intermediates, and (iv) formation of molecular hydrogen, alkene, or alkane subunits via formal β-H or β-alkyl migrations and subsequent losses of the so-formed neutral ligands.

Despite a wealth of experimentally based information on the elementary steps operative in remote functionalization, explicit information on structures and energetics of intermediates and transition structures by experimental means alone is, however, so far quite scarce if not absent for systems as complex as, for example, a nonanitrile/M<sup>+</sup>. In this respect, quantum chemical calculations provide a complementary tool to provide this kind of information if an appropriate computational strategy is applied.

To this end, we have performed a comprehensive theoretical study of the nonanitrile/M<sup>+</sup> system (M = Fe, Co). This particular nitrile was chosen because its chain length is sufficient to allow for competing bond activation at various positions,<sup>4</sup> while its size is not too large for a theoretical treatment. Due to the nature of the calculations, the organization of the paper is such that we will first describe the computational strategy applied that is appropriate for a treatment of open-shell, coordinatively unsaturated transition-metal complexes of this size. Afterward the theoretical results for nonanitrile/M<sup>+</sup> will be discussed, and then the predictive potential of the computational approach will be tested by an experimental study of the Fe<sup>+</sup> and Co<sup>+</sup> complexes of appropriately labeled model compounds. Finally, interpretations of some previous investigations will be analyzed with regard to the present findings, and the implications of this discussion will enable the formulation of a more general concept of remote functionalization in the gas phase.

## Computational Strategy

Even if only qualitative accuracy is desired, both the near degeneracy of states and the substantial relevance of dynamic electron correlation require rather sophisticated methods when open-shell transition-metal compounds are treated in the framework of conventional *ab initio* molecular orbital theory. Hence, the application of these methods is usually restricted to molecular ensembles much smaller than nonanitrile/M<sup>+</sup> or to coordinatively saturated transition-metal complexes. As an alternative, promising route for an accurate and yet computationally efficient treatment of such systems, density functional theory (DFT)<sup>10</sup> and, in particular, DFT/Hartree–Fock (HF) hybrid methods<sup>11</sup> have recently attracted considerable attention. These methods combine very appealing computational demands with satisfactory descriptions of open-shell organometallic species.<sup>12</sup> Recently, we applied a DFT/HF hybrid scheme<sup>13</sup> to analyze in detail the C–H and C–C bond activation pathways in the systems [Fe,C<sub>2</sub>,H<sub>6</sub>]<sup>+</sup>,<sup>13b</sup> [Co,C<sub>2</sub>,H<sub>6</sub>]<sup>+</sup>,<sup>13c</sup> and [Fe,C<sub>3</sub>,H<sub>8</sub>]<sup>+</sup>.<sup>13d</sup> With respect to C–H and C–C bond activation of alkanes by the bare metal cations Fe<sup>+</sup> and Co<sup>+</sup>, these studies provided new insight into the reaction mechanisms at a molecular level. (i) The initial insertions of M<sup>+</sup> into either C–H or C–C bonds are energetically less demanding than the subsequent rearrangements. This finding is in marked contrast to the commonly accepted mechanistic picture that in the transformation of hydrocarbons by organometallic catalysts the initial C–H or C–C bond activation steps are rate determining. (ii) Although often proposed, theory rules out the existence of genuine dihydrido minima (H)<sub>2</sub>ML<sup>+</sup> (M = Fe, Co; L = hydrocarbon ligand) as intermediates along the respective C–H bond activation reaction coordinates; similarly, hydridomethyl intermediates (H)(CH<sub>3</sub>)ML<sup>+</sup> are hardly relevant for C–C bond activation.<sup>13,14</sup> (iii) Rather, concerted elimination steps directly connect the C–H and C–C insertion intermediates with the product com-

(7) (a) Eller, K.; Zummack, W.; Schwarz, H. *Int. J. Mass Spectrom. Ion Processes* **1990**, *100*, 803. (b) Eller, K.; Karrass, S.; Schwarz, H. *Ber. Bunsen-Ges. Phys. Chem.* **1990**, *94*, 1201. (c) Eller, K.; Karrass, S.; Schwarz, H. *Organometallics* **1992**, *11*, 1637. (d) For a complete transition-metal ion screening, see: Eller, K.; Schwarz, H. *Chem. Ber.* **1990**, *123*, 201.

(8) (a) Schröder, D.; Eller, K.; Schwarz, H. *Helv. Chim. Acta* **1990**, *73*, 380. (b) Schröder, D.; Eller, K.; Prüsse, T.; Schwarz, H. *Organometallics* **1991**, *10*, 2052. (c) Stöckigt, D.; Sen, S.; Schwarz, H. *Chem. Ber.* **1993**, *126*, 2553. (d) Stöckigt, D.; Sen, S.; Schwarz, H. *Organometallics* **1994**, *13*, 1465. (e) Raabe, N.; Karass, S.; Schwarz, H. *Chem. Ber.* **1994**, *127*, 261. (f) Tjelta, B. L.; Armentrout, P. B. *J. Am. Chem. Soc.* **1996**, *118*, 9652.

(9) (a) Hornung, G.; Schröder, D.; Schwarz, H. *J. Am. Chem. Soc.* **1995**, *117*, 8192. (b) Hornung, G.; Schröder, D.; Schwarz, H. *J. Am. Chem. Soc.* **1997**, *119*, 2273.

(10) (a) *Density Functional Methods in Chemistry*; Labanowski, J. K., Andzelm, J. W., Eds.; Springer: Heidelberg, 1991. (b) Ziegler, T. *Chem. Rev.* **1991**, *91*, 651. (c) *Modern Density Functional Theory: A Tool for Chemistry*; Seminario, J. M., Politzer, P., Eds.; Elsevier: Amsterdam, 1995.

(11) (a) Becke, A. D. *J. Chem. Phys.* **1993**, *98*, 5648. (b) Stephens, P. J.; Devlin, F. J.; Chabalowski, C. F.; Frisch, M. J. *J. Phys. Chem.* **1994**, *98*, 11623.

(12) See, for example: (a) Holthausen, M. C.; Heinemann, C.; Cornehl, H. H.; Koch, W.; Schwarz, H. *J. Chem. Phys.* **1995**, *102*, 4931. (b) Holthausen, M. C.; Mohr, M.; Koch, W. *Chem. Phys. Lett.* **1995**, *240*, 245. (c) Heinemann, C.; Schwarz, H.; Koch, W.; Dyall, K. G. *J. Chem. Phys.* **1996**, *104*, 4642. (d) Ricca, A.; Bauschlicher, C. W., Jr. *Chem. Phys. Lett.* **1995**, *245*, 150. (e) Ricca, A.; Bauschlicher, C. W., Jr. *Theor. Chim. Acta* **1995**, *92*, 123. (f) Ricca, A.; Bauschlicher, C. W., Jr. *J. Phys. Chem.* **1995**, *99*, 5922. (g) Blomberg, M. R. A.; Siegbahn, P. E. R.; Svensson, M. *J. Chem. Phys.* **1996**, *104*, 9546. (h) Barone, V. *Chem. Phys. Lett.* **1995**, *233*, 129. (i) Barone, V. *J. Phys. Chem.* **1995**, *99*, 11659. (j) Adamo, C.; Lelj, F. *Chem. Phys. Lett.* **1995**, *246*, 463. (k) Barone, V.; Adamo, C. *J. Phys. Chem.* **1996**, *100*, 2094. (l) Pavlov, M.; Blomberg, M. R. A.; Siegbahn, P. E. M.; Wesendrup, R.; Heinemann, C.; Schwarz, H. *J. Phys. Chem.*, **1997**, *101*, 1567.

(13) (a) Holthausen, M. C. Ph.D. Thesis, Technische Universität Berlin D83, 1996. (b) Holthausen, M. C.; Fiedler, A.; Schwarz, H.; Koch, W. *Angew. Chem., Int. Ed. Engl.* **1995**, *34*, 2282; *J. Phys. Chem.* **1996**, *100*, 6236. (c) Holthausen, M. C.; Koch, W. *J. Am. Chem. Soc.* **1996**, *118*, 9932. (d) Holthausen, M. C.; Koch, W. *Helv. Chim. Acta* **1996**, *79*, 1939.

(14) Hendrickx, M.; Ceulemans, M.; Vanquickenborne, L. *Chem. Phys. Lett.* **1996**, *257*, 8.

plexes, e.g.,  $(H_2)ML^+$  or  $(CH_4)ML^+$ , via rate-determining, multicentered transition structures.<sup>13,15</sup>

While such a theoretical approach would also seem most appropriate for the current study, a few attempts to perform geometry optimizations on the nonanitrile/ $M^+$  systems employing the HF/DFT hybrid methods quickly revealed that the necessary amount of computer time for this project is prohibitive. Geometry optimizations, and in particular transition structure searches, on systems of this size and flexibility appear virtually impossible at this level of theory, even using reasonably modern computer hardware, which we can access (see below).

Therefore, the current computational investigation requires a reasonable compromise between various levels of theory. Among the several alternative DFT implementations available to us, the DGauss<sup>16</sup> program was found to be most efficient for geometry optimizations of local minima of nonanitrile/ $M^+$  complexes at the nonlocal DFT level of theory. A few test calculations for the  $[Fe, C_2, H_6]^+$  system revealed that the geometries obtained with the BLYP<sup>17</sup> functional showed nice agreement with those resulting from our former B3LYP<sup>11</sup> optimizations employing the Gaussian92/DFT program,<sup>18</sup> if the standard ECP/DZVP basis sets are used. However, the DGauss program does not offer any DFT/HF hybrid functional, and our previous studies have demonstrated that DFT alone is not adequate for an energetic description of unsaturated transition-metal ions.<sup>12,13</sup> Therefore, we decided to use BLYP geometries obtained with DGauss for single-point energy calculations with B3LYP using Gaussian92/DFT in order to evaluate the energetics with a quality comparable to that of the former studies on the alkane/ $M^+$  systems.<sup>13</sup>

Unfortunately, this approach was not feasible for transition structures (TSs); in fact, we have not been able to converge any TS using the transition structure search routines of DGauss. However, our previous studies<sup>12</sup> revealed that the PES (potential energy surface) is usually quite flat in the vicinity of stationary points, such that small deviations from properly optimized geometric parameters should hardly change the energetics. Together with the large structural similarities of comparable stationary points on the three alkane/ $M^+$  PESs investigated so far,<sup>13</sup> these findings led us to the idea to adopt the structural characteristics of the TSs localized in the alkane/ $M^+$  systems for the study of nonanitrile/ $M^+$ . Thus, instead of explicitly optimizing the transition structures at the BLYP level of theory, we constructed *model transition structures* for C–H and C–C bond activations in larger nitriles, by fixing the geometric parameters of the atoms characterizing the TS to those obtained with B3LYP for the alkane/ $M^+$  systems, while completely optimizing the remaining

degrees of freedom without any further constraint using the efficient DGauss program. Again, single-point energy calculations at the B3LYP level of theory were performed subsequently. Although such a scheme neglects certain cooperative effects (i.e., structural changes within the fixed moiety due to steric repulsion and/or electrostatic interactions of the metal ion with the aliphatic chain), the consequences for the computed relative energies are expected to be insignificant as these cooperative effects apply equally for all TSs and, hence, should cancel out.

An additional conceptual problem arises from the presence of the highly flexible alkyl chain in nonanitrile/ $M^+$ . While it is reasonable to assume that the global minimum in the conformational space of the uncoordinated nitrile is an *all-trans* conformation of the methylene units, a meaningful determination of the relative energies of the stationary points on the PES of nonanitrile complexes with  $Fe^+$  or  $Co^+$  ions is possible only after addressing the conformational multiple minimum problem of the aliphatic chain. As several hundreds of local geometry optimizations have to be performed in order to identify the global minimum of a system of the size of a nonanitrile/ $M^+$ , a quantum mechanical approach is not practical. Therefore, the conformational searching routines implemented in the program Spartan<sup>19</sup> in combination with the MM3 force field<sup>20</sup> were used in order to locate the lowest energy conformation of the aliphatic chain for each of the minima/model TSs investigated in this study. Force field calculations are particularly well suited for this kind of conformational analysis, since programs like MM3 have been explicitly parameterized for an accurate description of conformational effects in hydrocarbons. The energetically most stable conformers have then been used for the subsequent local geometry optimizations at the BLYP level of theory.

### Computational and Experimental Details

As outlined in the previous section, the input geometries for the *ab initio* calculations were generated by conformational searches with MM3. In these calculations, all metal/non-metal bond lengths were fixed to those resulting from our previous B3LYP investigations of the HCN/ $M^+$  and ethane/ $M^+$  systems for  $M = Fe$  and  $Co$ .<sup>13,21</sup> Next, all C–C–C bond angles were incremented systematically by  $60^\circ$ , the resulting pool of input geometries was submitted to subsequent geometry optimizations, and the conformers generated were then sorted according to the MM3 energies. These calculations have been performed for all structural isomers under investigation, i.e., initial encounter complexes, C–H and C–C bond insertion species, and model transition structures. In some cases, however, the conformational analysis resulted in several conformers very similar in energy and not related to each other by symmetry operations. Among these conformers we have chosen those for subsequent calculations that showed the largest structural similarities with lowest energy conformations of isomers, for which conformational searching revealed only one, unique lowest energy minimum. While such a

(15) (a) van Koppen, P. A. M.; Brodbelt-Lustig, J.; Bowers, M. T.; Dearden, D. V.; Beauchamp, J. L.; Fisher, E. R.; Armentrout, P. B. *J. Am. Chem. Soc.* **1991**, *113*, 2359. (b) van Koppen, P. A. M.; Kemper, P. R.; Bowers, M. T. *J. Am. Chem. Soc.* **1992**, *114*, 10941. (c) van Koppen, P. A. M.; Bowers, M. T.; Fisher, E. R.; Armentrout, P. B. *J. Am. Chem. Soc.* **1994**, *116*, 3780.

(16) DGauss 2.3, Cray Research, Inc. 1994.

(17) (a) Becke, A. D. *Phys. Rev. A* **1988**, *33*, 3098. (b) Lee, C.; Yang, W.; Parr, R. G. *Phys. Rev. B* **1988**, *37*, 785.

(18) GAUSSIAN92-DFT Rev. F.2: Frisch, M. J.; Trucks, G. W.; Schlegel, H. B.; Gill, P. M. W.; Johnson, B. G.; Wong, M. W.; Foresman, J. B.; Robb, M. A.; Head-Gordon, M.; Replogle, E. S.; Gomperts, R.; Andres, J. L.; Raghavachari, K.; Binkley, J. S.; Gonzales, C.; Martin, R. L.; Fox, D. J.; Defrees, D. J.; Baker, J.; Stewart, J. J. P.; Pople, J. A., Gaussian Inc.: Pittsburgh, PA, 1992.

(19) Spartan 3.0, Wavefunction, Inc., 18401 Von Karman Ave., Suite 370, Irvine, CA 92715.

(20) (a) Allinger, N. L., Yuh, Y. H., Lii, J.-H. *J. Am. Chem. Soc.* **1989**, *111*, 8551. (b) Lii, J.-H., Allinger, N. L. *J. Am. Chem. Soc.* **1989**, *111*, 8566. (c) *Ibid.* **1989**, *111*, 8576. (d) Allinger, N. L., Rahman, M., Lii, J.-H. *J. Am. Chem. Soc.* **1990**, *112*, 8293. (e) MM3 is a further development of the program MM2: Allinger, N. L. *J. Am. Chem. Soc.* **1977**, *99*, 8127.

(21) (a) Reference 13a. (b) Holthausen, M. C.; Koch, W., unpublished results.

procedure does not represent a strict systematic search for "global" minima in the conformational space of a given structural isomer, we do not expect a significant source of error here. This reasoning is based on the negligible energy differences of the low-energy conformers (below 0.2 kcal mol<sup>-1</sup> at the MM3 level of theory), as compared to other errors resulting from (i) the fixation of conformational characteristics in the transition structures and (ii) the previously<sup>12,13</sup> documented errors of the B3LYP functional in energy calculations.

The set of structures emerging from the conformational analysis was subsequently subjected to further geometry optimizations with the DGauss program using the BLYP functional in combination with the ECP/DZVP basis sets for all non-hydrogen atoms. Unconstrained geometry optimizations have been performed for all minimum structures. For the model transition structures (see above), the Cartesian coordinates of the atoms directly involved in the rearrangement were fixed, while optimizing all other degrees of freedom. The fixed geometry data were taken from the corresponding TSs from our previous studies on the alkane/M<sup>+</sup> systems.<sup>13</sup> All optimizations were performed by employing the standard medium convergence criteria of DGauss. The energies reported below were then obtained by performing single-point energy calculations on the DGauss-optimized structures using the B3LYP hybrid functional implemented in the program Gaussian92/DFT.<sup>11</sup> In these calculations, a (14s9p5d) → (8s4p2d) [62111111|3312|41] contraction of the all-electron basis set of Wachters<sup>22</sup> supplemented with d<sup>23</sup> and p-functions (Fe, α = 0.1150; Co, α = 0.1413) for the metal atoms, and standard D95\*\* basis sets were used for all non-metal atoms; the same combination of basis sets has been used in our previous B3LYP studies.<sup>13</sup> For all single-point energy calculations, tight SCF convergence criteria and the fine grid integration grid size option as implemented in Gaussian92/DFT, have been employed.

Throughout the theoretical study, we have assumed quartet and triplet spin states for Fe<sup>+</sup> and Co<sup>+</sup> complexes, respectively. Further, the combination of molecular modeling with *ab initio* calculations cannot provide vibrational frequencies, and thus zero-point vibrational energy corrections are not possible. All calculations have been performed on IBM/RS 6000 workstations and on a CRAY-J932/16/8192 mainframe of the Konrad-Zuse Zentrum für Informationstechnik Berlin.

The experiments were performed by using a modified VG ZAB/HF/AMD four-sector mass spectrometer of BEBE configuration (B stands for magnetic and E for electric sectors) which has been previously described in detail.<sup>24</sup> Briefly, the metal complexes were generated in a chemical ionization source (CI, repeller voltage ~0 V) by 100 eV electron bombardment of an approximately 2:1 mixture of Fe(CO)<sub>5</sub> or Co(CO)<sub>3</sub>(NO), respectively, and the aliphatic nitrile of interest. The ions were accelerated to 8 keV kinetic energy and mass-selected by means of B(1)/E(1) at a resolution of  $m/\Delta m = 2000$ –3000 to provide separation of isobaric ions. Unimolecular fragmentations of metastable ions occurring in the field-free region preceding B(2) were recorded by scanning this sector; the last sector E(2) was not used in this study. All spectra were accumulated and on-line processed with the AMD-Intetra data system; 10–20 scans were averaged in order to improve the signal-to-noise-ratio and to account for statistical error. The data for the isotopologous nonanitriles are the averages of several independent measurements. The error of the averaged relative intensities in the MS/MS experiments is

estimated as ±2%.<sup>25</sup> While reactions of electronically excited metal ions may obscure the results for metastable ions, previous studies of nitrile/M<sup>+</sup> systems<sup>26</sup> as well as the relatively high pressure that prevails in the CI source suggest that excited states of M<sup>+</sup> ions are unlikely to participate in the reactions described below.<sup>27</sup>

For an estimation of the bond dissociation energies (BDEs) of RCN–M<sup>+</sup> for M = Fe and Co, we applied the kinetic method according to Cooks and co-workers.<sup>28</sup> To this end, mixed bisligand complexes of the type M(L)(L')<sup>+</sup> were generated by chemical ionization, and the fragments M(L)<sup>+</sup> and M(L')<sup>+</sup> formed upon unimolecular decomposition of mass-selected M(L)(L')<sup>+</sup> complexes were monitored. Then, the ratio M(L)/M(L')<sup>+</sup> was converted to ΔBDE assuming a temperature of 473 K,<sup>29</sup> using BDE(M<sup>+</sup>–CO), BDE(M<sup>+</sup>–C<sub>2</sub>H<sub>4</sub>), and BDE(M<sup>+</sup>–C<sub>6</sub>H<sub>6</sub>) as reference anchor points.<sup>29,30</sup> For nonanitrile/M<sup>+</sup>, we obtain BDE(Fe<sup>+</sup>–nonanitrile) = 48 ± 3 kcal mol<sup>-1</sup> and BDE(Co<sup>+</sup>–nonanitrile) = 56 ± 3 kcal mol<sup>-1</sup>; complete details of this study including various nitrile ligands will be published elsewhere.<sup>31</sup>

The unlabeled C<sub>9</sub>–C<sub>11</sub> nitriles were commercially available and used without further purification. The isotopologs were synthesized by standard laboratory procedures, i.e., copper-mediated cross coupling<sup>32</sup> of labeled Grignard reagents with α,ω-dibromoalkanes and subsequent nucleophilic substitution of the so-formed 1-bromoalkanes with potassium cyanide in dimethyl sulfoxide.<sup>33</sup> The Grignard reagents were obtained from alkyl bromides which were made from the corresponding acids or aldehydes by reduction with lithium aluminum hydride (or deuteride) and subsequent, *in situ* bromodehydroxylation with aqueous HBr (48%). The final products were purified by either distillation or preparative gas chromatography and fully characterized by spectroscopic means. The purity of the compounds, the location, and the degree of deuterium incorporation were confirmed by <sup>1</sup>H NMR and mass spectrometry.

## Results and Discussion

This section is organized according to the development of the project. Starting points were the very first papers on remote functionalization in the gas phase,<sup>34</sup> in which different regioselectivities for bond activation of alkyl nitriles by Fe<sup>+</sup> and Co<sup>+</sup> were reported. The aim of the present study is to unravel both the origin of these effects and the underlying principles. In this respect, the following problems are of particular interest: (i) To what extent does the nature of the docked metal ion influence the trajectory of approach for C–H and C–C bond activation? (ii) What is the role of the chain length in the formation of the intermediates and the associated transition structures? (iii) Which position is favored for

(25) This estimate is based on the maximum deviation from the average of two independent sets of measurements of the nonanitrile isotopologs.

(26) Eller, K.; Schwarz, H. *Int. J. Mass Spectrom. Ion Processes* **1989**, *93*, 243.

(27) (a) Schulze, C.; Schwarz, H. *Chimia* **1988**, *42*, 297. (b) Armentrout, P. B. *Science* **1991**, *251*, 175. (c) Schalley, C.; Schröder, D.; Schwarz, H. *J. Am. Chem. Soc.* **1994**, *116*, 11089.

(28) Cooks, R. G.; Patrick, J. S.; Kotiqah, T.; McLuckey, S. A. *Mass Spectrom. Rev.* **1994**, *13*, 287.

(29) Schröder, D.; Schwarz, H. *J. Organomet. Chem.* **1995**, *504*, 123.

(30) (a) Kickel, B. L.; Armentrout, P. B. In *Organometallic Ion Chemistry*; Freiser, B. S., Ed.; Kluwer: Dordrecht, The Netherlands, 1996; p 1. (b) Meyer, F.; Khan, F. A.; Armentrout, P. B. *J. Am. Chem. Soc.* **1995**, *117*, 9740.

(31) Hornung, G.; Schwarz, H., unpublished results.

(32) Tamura, M.; Kochi, J. *Synthesis* **1971**, 303.

(33) (a) Smiley, R. A.; Arnold, C. *J. Org. Chem.* **1960**, *25*, 257. (b) Friedmann, L.; Shetcher, H. *J. Org. Chem.* **1960**, *25*, 877.

(34) (a) Lebrilla, C. B.; Schulze, C.; Schwarz, H. *J. Am. Chem. Soc.* **1987**, *109*, 98. (b) Lebrilla, C. B.; Drewello, T.; Schwarz, H. *J. Am. Chem. Soc.* **1987**, *109*, 5639. (c) Lebrilla, C. B.; Drewello, T.; Schwarz, H. *Int. J. Mass Spectrom. Ion Processes* **1987**, *79*, 287.

(22) Wachters, A. J. H. *J. Chem. Phys.* **1970**, *52*, 1033.

(23) Hay, P. J. *J. Chem. Phys.* **1977**, *66*, 4377.

(24) (a) Srinivas, R.; Sülzle, D.; Weiske, T.; Schwarz, H. *Int. J. Mass Spectrom. Ion Processes* **1991**, *107*, 368. (b) Srinivas, R.; Sülzle, D.; Koch, W.; DePuy, C. H.; Schwarz, H. *J. Am. Chem. Soc.* **1991**, *113*, 5970.

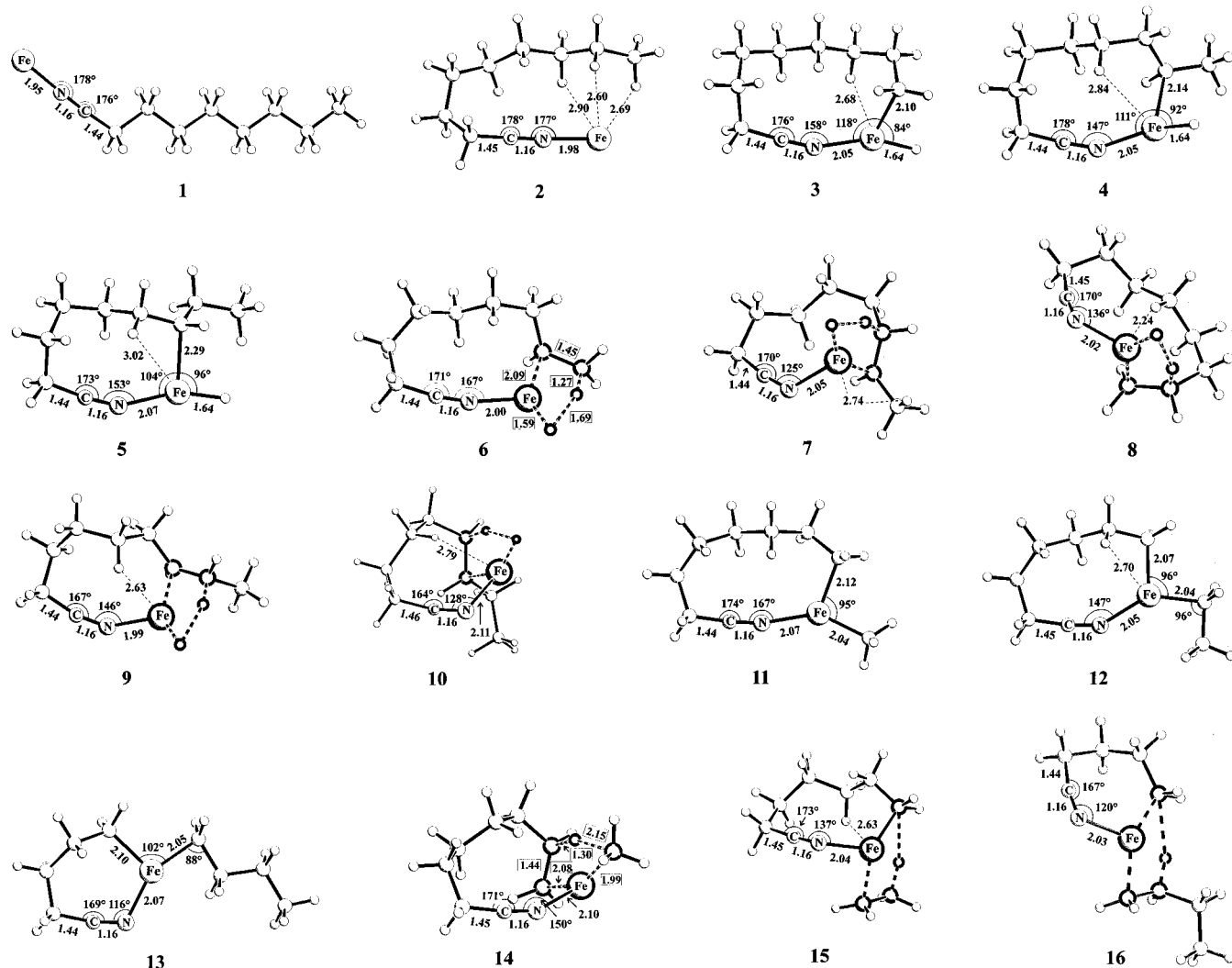


**Figure 1.** Geometries of the intermediates **1–16** relevant in C–H and C–C bond activation of nonanitrile/ $M^+$  for  $M = Fe$ . For the sake of clarity, only selected bond lengths and angles are given; also, the very similar structural features for  $M = Co^+$  are not shown. The atoms, which have been held fixed in the geometry optimizations of the model transition structures, are emphasized in bold.

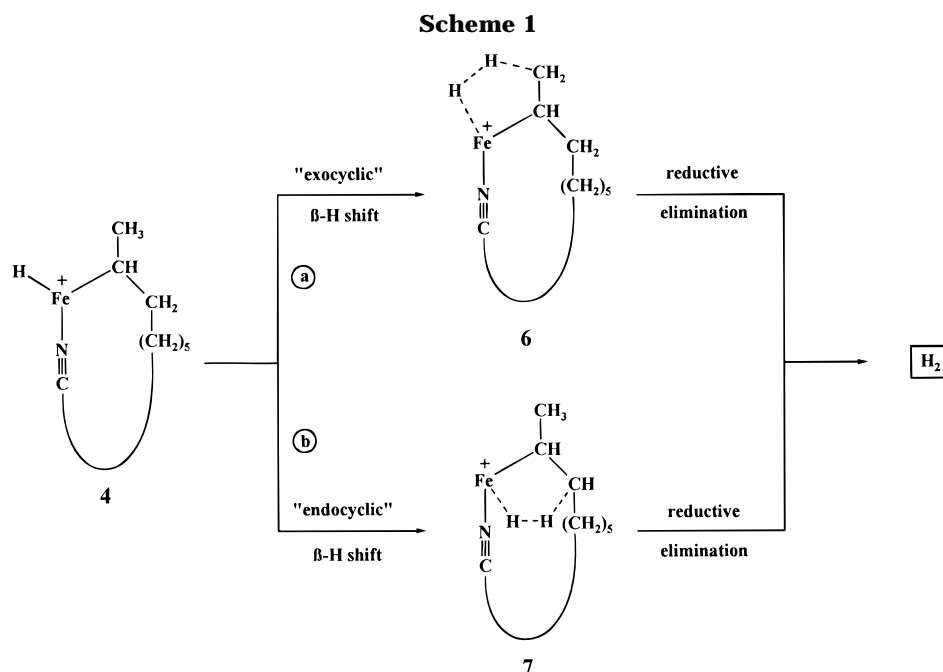
the primary C–H bond activation step? (iv) Is the C–H bond insertion of the metal ion followed by an endocyclic or an exocyclic  $\beta$ -H shift?

After having completed the theoretical studies, the predictive capability of the approach was tested by the experimental investigation of appropriate  $RCN-M^+$  ( $M = Fe, Co$ ) complexes for nonanitrile and its isotopologs. Finally, the combined results of this investigation lead to new interpretations of previous experimental findings; further, they have some implications toward a more general understanding of remote functionalization in the gas phase.

**A. Theoretical Results.** The geometries of all structures investigated are depicted in Figure 1 for  $M = Fe$ . Very similar geometries evolve for the cobalt species, and the major differences between the two metals are already present in the basic ethane/ $M^+$  systems.<sup>13</sup> Therefore, we will address only the geometries of the nonanitrile/ $Fe^+$  system and refrain from a discussion of the geometrical features of the cobalt analogs.

**a. Nonanitrile/ $Fe^+$ .** Let us first consider the initial interaction of the iron cation with nonanitrile. The complexation of the metal ion liberates the energy

necessary for further transformations. Although an *all-trans* conformation of methylene groups corresponds to the global minimum of isolated nonanitrile, the *end-on* complexation of the metal cation to the cyano group; i.e., **1**, does not represent the most stable structure in this region of the PES. Rather, folding of the alkyl chain allows for interaction of the metal ion with both the cyano group and remote C–H bonds leading to the cyclic structure **2**, which is 4 kcal mol<sup>-1</sup> lower in energy than **1**. The coordination mode in **2** can be described in terms of internal solvation and, hence, leads to an immobilization of the otherwise flexible alkyl chain. By such, a spatial region is predetermined for the subsequent regioselective C–H and C–C bond activation. Obviously, coordination of the metal at the C(7), C(8), and C(9) positions is particularly preferred: the optimized geometry of **2** shows an almost linear, unperturbed, Fe–N–C moiety, and deviations from the *all-trans* conformation of the chain occur only at C(2)–C(3), C(3)–C(4), and C(4)–C(5); i.e., the bonds which are responsible for the recoil of the alkyl chain toward the metal center. All attempts failed to find conformations, in which the metal interacts with C–H bonds at positions closer to the cyano group, i.e., below C(7). Even when starting



from reasonably preoptimized geometries, in which the metal was forced to interact with inner positions of the chain by geometry constraints, subsequent constraint-free optimizations at the BLYP level of theory led directly to conformers **1** or **2**, respectively. With respect to the entrance channel  $\text{Fe}^+(\text{}^6\text{D}) + \text{C}_8\text{H}_{17}\text{CN}$ , complex **2** is bound by  $66 \text{ kcal mol}^{-1}$ . Considering the B3LYP error of  $9 \text{ kcal mol}^{-1}$  in the atomic  $\text{Fe}^+(\text{}^6\text{D}/\text{}^4\text{F})$  splitting,<sup>13,14</sup> a corrected bond dissociation energy of  $57 \text{ kcal mol}^{-1}$  is our best theoretical estimate. In view of the known tendency of DFT methods<sup>35</sup> to overestimate BDEs by  $5\text{--}10 \text{ kcal mol}^{-1}$  as well as the neglect of zero-point vibrational and thermal energy contributions, this value is in good qualitative agreement with the experimental estimate of  $48 \pm 3 \text{ kcal mol}^{-1}$  (see below).

After formation of the encounter complex **2**, the metal center already interacts with the region within the aliphatic chain, in which subsequently C–H and C–C insertion can take place. Commencing with the C–H bond activation pathways, we found three minima **3**, **4**, and **5** which result from insertions into the C–H bonds at C(9), C(8), and C(7), respectively. As our former studies on the  $\text{Fe}^+$ -mediated C–H bond activations in ethane and propane revealed that the energies of C–H bond insertion minima are very similar to the relative energies of the preceding C–H insertion TSs, we may consider the C–H insertion minima **3**, **4**, and **5** as "Hammond-analogs" of the corresponding TSs; thus, computationally demanding efforts for an explicit modeling of the latter are avoided. With respect to **2**, the relative energies of **3**, **4**, and **5** are 17, 14, and  $20 \text{ kcal mol}^{-1}$ , respectively. These figures are in good agreement with our earlier investigations on the  $[\text{Fe}, \text{C}_2, \text{H}_6]^+$  and  $[\text{Fe}, \text{C}_3, \text{H}_8]^+$  systems,<sup>13</sup> in which the C–H insertion minima are 18 (ethane), 19 (propane,  $\beta$ -C–H), or  $20 \text{ kcal mol}^{-1}$  (propane,  $\alpha$ -C–H) less stable than the corresponding encounter complexes.

Starting from the most stable insertion product **4**, reductive elimination of dihydrogen can occur in two different directions (Scheme 1), i.e., breaking of a

terminal C–H bond in an exocyclic manner (pathway a) or transfer of an internal hydrogen in an endocyclic fashion (pathway b). The calculations reveal a significant difference in energy between both structures and clearly favor the exocyclic pathway involving the model transition structure **6** versus the endocyclic route via TS **7**: TS **6** is computed to be  $24 \text{ kcal mol}^{-1}$  higher in energy than **2**, but yet is  $10 \text{ kcal mol}^{-1}$  more stable than TS **7**. Both TS **6** and TS **7** correspond to multicentered transition structures for the concerted elimination of molecular hydrogen from the insertion minima. However, formation of the endocyclic TS **7** is accompanied by a significant increase of strain in the aliphatic backbone, which becomes particularly evident by the stronger deviation from a linear Fe–N–C arrangement in TS **7** as compared to TS **6**, i.e.,  $125$  versus  $167^\circ$ . Therefore, dehydrogenation of nonanitride/ $\text{Fe}^+$  occurs preferentially via path a although it leads to a less stable product as compared to path b, i.e., an iron complex of a terminal versus that of an internal cyano alkene.

Yet another pathway for the elimination of molecular hydrogen from the terminal positions C(8) and C(9) involves TS **8**, the model transition structure for an endocyclic elimination step following the initial C(9)–H insertion intermediate **3**. Relative to the encounter complex **2**, TS **8** is located  $33 \text{ kcal mol}^{-1}$  higher in energy. Thus, as compared to the exocyclic elimination of H<sub>2</sub> via TS **6**, the endocyclic elimination via TS **8** is similarly disfavored as the endocyclic elimination via TS **7**.

Finally, the C(7)–H insertion minimum **5** can undergo analogous reactions. The exocyclic elimination of H<sub>2</sub> from C(7) and C(8) via TS **9** is associated with a moderate barrier of  $29 \text{ kcal mol}^{-1}$  relative to **2**. In comparison to TS **6**, the higher activation energy associated with exocyclic dehydrogenation of **5** via TS **9** can be traced back to increasing strain in the TS with decreasing sizes of the fused rings, i.e., the Fe–N–C angle changes from  $167^\circ$  in TS **6** to  $146^\circ$  in TS **9**. Alternatively, **5** can lead to an endocyclic elimination

(35) Ziegler, T.; Li, J. *Can. J. Chem.* **1994**, *72*, 783.

of hydrogen involving C(7) and C(6) via the model TS **10**. However, this pathway is again significantly less favorable (38 kcal mol<sup>-1</sup> relative to **2**).

In summary, the energetic order of the investigated model transition structures can be qualitatively understood as a consequence of several cooperative effects, i.e., ring strain, *exo*- versus endocyclic elimination, and activation of primary or secondary C–H bonds. Note, however, that the decrease of the ring sizes, and thus the increase of strain, is partially compensated by internal solvation of the metal cation in these more compact TSs, i.e., additional Fe–H interactions in TSs **8**, **9**, and **10**, respectively, while such interactions (i.e., H contacts closer than 3 Å) do not exist in the less congested TSs **6** and **7**. Yet, the energetically least demanding route for dehydrogenation of nonanitrile/Fe<sup>+</sup> proceeds via an exocyclic elimination involving TS **6**. This finding agrees well with the previously reported preference of “bare” Fe<sup>+</sup> ions to activate longer aliphatic nitriles at remote positions and also with the new experimental findings (see below). The exocyclic elimination of H<sub>2</sub> from C(7) and C(8) via TS **9** is less favorable by 5 kcal mol<sup>-1</sup> but is still preferred by ~5 kcal mol<sup>-1</sup> as compared to the lowest endocyclic elimination pathways via TS **7** and TS **8**, which are quite similar in energy and which also involve C(7)/C(8) and C(8)/C(9), respectively. However, dehydrogenation of internal positions is much less favorable, and therefore, theory predicts that it will hardly play a role in the experiment.

Let us now turn to the analysis of the C–C bond activation in the nonanitrile/Fe<sup>+</sup> system. Commencing with the formation of the encounter complex **2**, C–C bond activation can take place directly by insertion of iron into the C(8)–C(9) and C(7)–C(8) bonds, respectively, which are easily accessible for the metal without major geometrical changes of the remaining part. The corresponding insertion minima **11** and **12** are both located 7 kcal mol<sup>-1</sup> above the relative energy of **2** and thus are fairly more stable than the corresponding C–H bond insertion intermediates **4** and **5** by 7 and 13 kcal mol<sup>-1</sup>, respectively. The higher stability of the C–C insertion species agrees nicely with our findings for the propane/Fe<sup>+</sup> system<sup>13</sup> for which the C–C insertion intermediate is more than 10 kcal mol<sup>-1</sup> lower in energy than the  $\alpha$ - and  $\beta$ -C–H bond-inserted structures. In order to account for other C–C bond activation processes, we extended our study to isomer **13** in which the metal has inserted into the C(5)–C(6) bond, i.e., the innermost position within the aliphatic chain for which C–C bond activation of decanitrile/Fe<sup>+</sup> has been observed experimentally.<sup>34b</sup> In fact, our calculations reveal that **13** corresponds to a relatively stable minimum which is located 13 kcal mol<sup>-1</sup> above the relative energy of **2**. Thus, this C–C insertion product is still lower in energy as compared to any of the C–H bond insertion species **3**–**5**.

Next, starting from **11**, **12**, and **13** we investigated the activation barriers connected with the subsequent reductive eliminations of methane, ethene, and 1-butene, respectively. As a building block for the constrained geometry optimizations of the model TSs, we adopted the geometrical features from the transition structure for elimination of methane in the propane/Fe<sup>+</sup> system.<sup>13a,d</sup> The resulting model transition structure associated with the elimination of methane, TS **14**, is located 30 kcal

mol<sup>-1</sup> above the relative energy of **2**, thus, in energetic terms in the energetic regime of the dehydrogenation pathways. A slightly higher activation barrier of 34 kcal mol<sup>-1</sup> with respect to **2** results for the reductive elimination of ethene from **12** via TS **15**. Finally, the calculations predict an activation barrier of 30 kcal mol<sup>-1</sup> connected with the loss of 1-butene via TS **16**. In light of these results, the reductive elimination of methane and 1-butene are connected with similar barrier heights as is the exocyclic elimination of H<sub>2</sub> from C(7)/C(8), and thus losses of methane and butene should be more probable than those of ethene. Further, if elimination of methane or butene is observed experimentally in the fragmentation of metastable nonanitrile/Fe<sup>+</sup>, a significant amount of the dehydrogenation should stem from positions C(7) and C(8). We do not, however, have a straightforward explanation of why the loss of C<sub>2</sub>H<sub>4</sub> is the most abundant process reported in previous experimental studies on Fe<sup>+</sup>-mediated activation processes of longer nitriles. We calculate the corresponding process via TS **15** to be 4 kcal mol<sup>-1</sup> more energy demanding than the other two C–C bond activation processes investigated. However, the choice of the TS associated with elimination of methane from the propane/Fe<sup>+</sup> system as the guiding structure in the construction of model TS **15** is somewhat problematic. Rather, the TS for C–C bond cleavage in butane/Fe<sup>+</sup> would represent an adequate model TS, but this system has not explicitly been studied so far. Thus, for the time being the calculated activation barrier associated with loss of ethene may be somewhat overestimated.

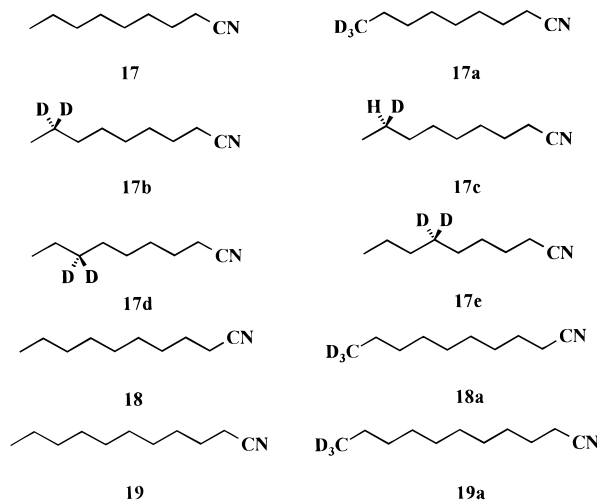
**b. Nonanitrile/Co<sup>+</sup>.** In order to examine the previously deduced preference for bond activation of aliphatic nitriles at C(7) in the case of Co<sup>+</sup> rather than at C(8) for Fe<sup>+</sup>,<sup>34,36a</sup> we performed an analogous series of computations on the model transition structures of the respective nonanitrile/Co<sup>+</sup> system. For these calculations we used the geometrical characteristics of the transition structure for the concerted elimination of molecular hydrogen optimized in our study on the [Co,C<sub>2</sub>,H<sub>6</sub>]<sup>+</sup> system. As for the nonanitrile/Fe<sup>+</sup> system, the initial interaction of the cobalt atom leads to a cyclic structure **2'**, in which the metal interacts with the hydrogen atoms at C(7), C(8), and C(9). Again, we were unable to find local minima different from **2'**, in which the metal interacts with methylene groups closer to the nitrile function than C(7). With regard to the Co<sup>+</sup>(<sup>3</sup>F) + C<sub>8</sub>H<sub>17</sub>CN asymptote, we compute a binding energy of 64 kcal mol<sup>-1</sup> for the encounter complex which is also in reasonable agreement with the experimental estimate of 56 ± 3 kcal mol<sup>-1</sup> (see below). Good agreement is also found for the theoretically calculated difference (7 kcal mol<sup>-1</sup>) in the binding energies of **2'** and the respective iron species **2** and the experimentally determined difference of 8 kcal mol<sup>-1</sup>. While in the optimized structure of **2'** the metal–hydrogen distances are slightly larger than in the corresponding iron complex **2**, the metal nitrogen distances are found to be identical for both systems. This result is interesting in that it rules out different geometric arrangements (i.e., different ring sizes due to different M–N bond lengths) in the initial encounter complexes of Fe<sup>+</sup> and Co<sup>+</sup> as the origin for the experimentally observed differences in the preferred activation position for both metal ions—a speculation put forward in earlier work.<sup>36a</sup>

The calculations performed on the model transition structures also lead to geometries that are generally very similar to the respective iron complexes. Furthermore, the calculations on the model transition structures of the cobalt analogs led to an unexpected result for the order of relative energies (with respect to **2'**): (**6'**) 26, (**7'**) 38, (**8'**) 36, (**9'**) 32, and (**10'**) 42 kcal mol<sup>-1</sup>. The comparison with the relative energies of the corresponding iron species (with respect to **2**: (**6**) 24, (**7**) 34, (**8**) 33, (**9**) 29, and (**10**) 38 kcal mol<sup>-1</sup>) does not show any preference for the activation of inner positions in the aliphatic chain, as was argued based on the former experimental studies. Rather, the resulting relative energies point to an even more pronounced tendency to eliminate H<sub>2</sub> from C(8) and C(9) positions in an exocyclic fashion in nonanitrile/Co<sup>+</sup>—the energy difference to the energetically closest reaction channel via **7'** is slightly higher for the cobalt system as are the relative energies of all other computed model transition structures. This surprising result necessitates one to conclude that the differences between Fe<sup>+</sup>- and Co<sup>+</sup>-mediated C–H bond activations are not caused by a striking preference of the metal ions to insert into different chain positions. Instead, the calculations clearly predict that the most favorable trajectory of C–H bond activation corresponds to the exocyclic elimination of H<sub>2</sub> from C(8) and C(9) for both metal ions. The only distinctive difference revealed by theory concerns the generally elevated activation barriers for the Co<sup>+</sup> system as compared to that of Fe<sup>+</sup>; this trend is fully in line with the results of our previous studies on the ethane activation studies.<sup>13</sup>

The last two reaction pathways we assessed in our theoretical investigation are the reductive elimination of methane and ethene from the Co<sup>+</sup>/nonanitrile system. Because the Co<sup>+</sup>-mediated C–C bond activation of propane has not been examined so far, no geometric data for the transition structure for the methane elimination were available to us, we used instead the geometric data of the corresponding Fe<sup>+</sup> structures **13** and **14**, replaced the iron center with a cobalt atom, and performed the geometry optimizations by employing the same geometry constraints as for the iron systems. The resulting geometries did not show any significant changes (larger than 0.05 Å in bond lengths or 1° in bending angles) in the reoptimized geometric parameters as compared to the optimized structures of **13** and **14**. The resulting relative energies (**(13')** 36, **(14')** 40 kcal mol<sup>-1</sup>) are both higher by 6 kcal mol<sup>-1</sup> than the corresponding iron species **13** and **14**. While this trend is again in agreement with our former studies on the ethane activation studies (here, the Co<sup>+</sup>-mediated CC activation is 10 kcal mol<sup>-1</sup> more demanding than the Fe<sup>+</sup>-mediated reaction), it is puzzling with respect to the earlier experimental finding that C–C bond cleavage is significantly more pronounced for the Co<sup>+</sup> complexes of nitriles as compared to the Fe<sup>+</sup> analogs.

**B. Experimental Results.** First, the BDEs of nonanitrile/M<sup>+</sup> (for M = Fe and Co) were estimated using Cooks kinetic method.<sup>28,29,31</sup> We obtain estimates of BDE(Fe<sup>+</sup>–nonanitrile) = 48 ± 3 kcal mol<sup>-1</sup> and BDE(Co<sup>+</sup>–nonanitrile) = 56 ± 3 kcal mol<sup>-1</sup>, respectively, which are in satisfying accordance with the theoretical predictions (see above). Further, these studies reveal that BDE(M<sup>+</sup>–nonanitrile) is significantly larger than BDE(M<sup>+</sup>–NCR) for R = H, CH<sub>3</sub>, and C<sub>2</sub>H<sub>5</sub>; for example,

Chart 1



in the case of Fe<sup>+</sup> the nonanitrile is ~5 kcal mol<sup>-1</sup> more strongly bound to the metal than propionitrile.<sup>31</sup> This finding is in excellent agreement with the computational result that, due to internal solvation of the metal cation by the alkyl chain, **2** is ~4 kcal mol<sup>-1</sup> more stable than the *all-trans* conformer **1**.

Our major intention was of course to assess the accuracy of the computational predictions with respect to the regioselectivities of C–H/C–C bond activations: With respect to an experimental verification/falsification, the results of the theoretical study for nonanitrile/M<sup>+</sup> can be summarized as follows: (i) C–H and C–C bond activations at the inner positions, i.e., ≤C(6), are negligible, and hence, no labeling experiments are required within this part of the alkyl chain. (ii) C–H bond activation at C(8) is most facile; therefore, the intramolecular kinetic isotope effect should be analyzed for this particular position. (iii) In order to evaluate to what extent the computed regioselectivities translates to higher alkane nitriles, the chain length needs to be extended further. By such it can be determined whether the preferential activation at C(8) is specific only for the nonanitrile system or whether it represents an intrinsic feature in the remote functionalization of nitriles by Fe<sup>+</sup> and Co<sup>+</sup> cations. Thus, for an experimental investigation of these problems, we synthesized the model substrates **17–19** (Chart 1).

In general, the types of products observed in the unimolecular decomposition of the isotopologous nitriles **17–19** complexed to “bare” Fe<sup>+</sup> and Co<sup>+</sup> ions in the gas phase are very similar, while the relative product abundances differ significantly depending on both the nitrile and the metal cation. According to the MI mass spectra, all these complexes follow three major unimolecular decomposition pathways: (i) dehydrogenation ( $\Delta m = 2$  amu), (ii) loss of methane ( $\Delta m = 16$  amu), and (iii) expulsion of the neutral olefins ethene ( $\Delta m = 28$  amu), propene ( $\Delta m = 42$  amu), and butene ( $\Delta m = 56$  amu), respectively. In the case of the metastable Co<sup>+</sup>/nonanitrile complexes, a fourth unimolecular decomposition pathway is observed which corresponds to the formation of neutral alkanes, such as ethane ( $\Delta m = 30$  amu), propane ( $\Delta m = 44$  amu), and butane ( $\Delta m = 58$  amu). Except for the relative product distributions, the latter processes represent the most apparent difference in the unimolecular fragmentations of the Fe<sup>+</sup> versus the analogous Co<sup>+</sup> complexes.



**Table 1. Mass Differences (amu) Observed in the Unimolecular Fragmentations of Isotopologous Fe<sup>+</sup> Complexes of 17–19<sup>a,b</sup>**

precursor	$\Delta m$															
	2	3	16	17	19	28	29	30	42	43	44	45	56	57	58	59
<b>17</b>	63		2			31			3				1			
<b>17a</b>	20	42			2			27				8				1
<b>17b</b>	3	62	4					26		4					1	
<b>17c</b>	45	23	3				23		2	3				1		
<b>17d</b>	53	7		1		32					6			1		
<b>17e</b>	65	1	2			27			4						1	
<b>18</b>	57		9			23			10				1			
<b>18a</b>	35	18			8			22				15				2
<b>19</b>	41		15			23			17				4			
<b>19a</b>	30	9			9			15				27				10

<sup>a</sup> Intensities are normalized to  $\sum_{\text{reactions}} = 100\%$ . <sup>b</sup> Reactions with intensities of <1% are omitted.

To render the discussion of our results more distinct, the organization of this section is such that we will first describe in detail the nonanitrile/Fe<sup>+</sup> system, followed by a brief discussion of the gas-phase chemistry of the corresponding Co<sup>+</sup> complexes with an emphasis on a comparison of the experimental and theoretical aspects concerning the regioselectivity of the dehydrogenation process. The experimental set of data reported for the decanitrile and the undecanitrile isotopologous transition-metal complexes of **18a** and **19a** will only be discussed as far as the regioselectivity of the neutral hydrogen loss is concerned.

**a. Nonanitrile/Fe<sup>+</sup>.** The gas-phase reactivity of “naked” Fe<sup>+</sup> ions with nonanitrile is characterized by the generation of three classes of neutral products, corresponding to the formation of hydrogen, methane, and small alkenes (Table 1). The isotope distribution patterns of all products agree well with the general mechanism for remote functionalization,<sup>4</sup> i.e., formal 1,2-elimination processes, and by referring to these previous studies, we will therefore not pursue these mechanistic aspects any further.

The MI mass spectra of the nonanitrile/Fe<sup>+</sup> complexes are dominated by dehydrogenation which amounts to 60–68% of all products formed, depending on the isotopologs studied. In several earlier investigations,<sup>36</sup> it was shown that the gas-phase dehydrogenation of Fe<sup>+</sup> complexes of linear aliphatic nitriles with up to seven carbon atoms proceeds exclusively from the  $\omega$  and the  $(\omega - 1)$  positions. However, with increasing chain length, insertion into internal C–H bonds is expected to begin to compete with the activation of the terminal positions. In fact, the data for the deuterium-labeled isotopologs of nonanitrile/Fe<sup>+</sup> clearly reveal that dehydrogenation involves the  $\omega/(\omega - 1)$  and the  $(\omega - 1)/(\omega - 2)$  positions, respectively; activation of internal positions is negligible, e.g., loss of HD from **17e**/Fe<sup>+</sup> hardly occurs.

In terms of a mechanistic analysis with regard to a comparison with the theoretical study, a more detailed analysis of the regioselectivity is indicated. In any attempt to derive intrinsic selectivities from data of labeled compounds, the possibility of isotopically sensi-

tive branching<sup>37</sup> must be considered in the evaluation. However, the amount of dehydrogenation (expressed as the sum of H<sub>2</sub> and HD losses) is similar for all isotopologous complexes studied here. Thus, in a first approximation we can assume that switching from dehydrogenation to the other reactions need not be included in the data analysis. Nevertheless, due to the obvious competition of activation of the various sites between C(6) and C(9), this type of analysis is not straightforward and must account for this competition as well as for the kinetic isotope effect (KIE) associated with loss of HD. For that purpose, we partitioned the experimentally observed H<sub>2</sub>/HD ratios for **17a–e**/Fe<sup>+</sup> according to the respective position of the isotope and the KIE (eqs 1a–1e), with  $\sum k_i = 1$  and assuming the

$$\text{H}_2/\text{HD} (\mathbf{17a}/\text{Fe}^+) = \text{KIE}[(k_{\text{C}(7)/\text{C}(8)} + k_{\text{C}(6)/\text{C}(7)})/k_{\text{C}(8)/\text{C}(9)}] \quad (1a)$$

$$\text{H}_2/\text{HD} (\mathbf{17b}/\text{Fe}^+) = \text{KIE}[k_{\text{C}(6)/\text{C}(7)}/(k_{\text{C}(8)/\text{C}(9)} + k_{\text{C}(7)/\text{C}(8)})] \quad (1b)$$

$$\text{H}_2/\text{HD} (\mathbf{17c}/\text{Fe}^+) = \text{KIE}[(k_{\text{C}(8)/\text{C}(9)} + k_{\text{C}(7)/\text{C}(8)} + 2k_{\text{C}(6)/\text{C}(7)})/(k_{\text{C}(8)/\text{C}(9)} + k_{\text{C}(7)/\text{C}(8)})] \quad (1c)$$

$$\text{H}_2/\text{HD} (\mathbf{17d}/\text{Fe}^+) = \text{KIE}[k_{\text{C}(8)/\text{C}(9)}/(k_{\text{C}(7)/\text{C}(8)} + k_{\text{C}(6)/\text{C}(7)})] \quad (1d)$$

$$\text{H}_2/\text{HD} (\mathbf{17e}/\text{Fe}^+) = \text{KIE}[(k_{\text{C}(8)/\text{C}(9)} + k_{\text{C}(7)/\text{C}(8)})/k_{\text{C}(6)/\text{C}(7)}] \quad (1e)$$

same KIE =  $k_{\text{H}_2}/k_{\text{HD}}$  for all positions in the chain. This deconvolution can be done by separating the relative rate constants for the various dehydrogenation sites, i.e.,  $k_{\text{C}(8)/\text{C}(9)}$  for the two terminal positions,  $k_{\text{C}(7)/\text{C}(8)}$  for the next two C–H bonds, and  $k_{\text{C}(6)/\text{C}(7)}$  as a representative for the dehydrogenation of inner positions of the chain.

Using the experimental figures reported in Table 1, we obtain a reasonable solution<sup>38</sup> for KIE = 2.0 together

(37) (a) Thibblin, A.; Ahlberg, P. *Chem. Soc. Rev.* **1989**, *18*, 209. (b) Taeger, J. C.; Morton, T. M. *J. Am. Chem. Soc.* **1996**, *118*, 9661. (c) Schalley, C. A.; Schröder, D.; Schwarz, H. *Int. J. Mass Spectrom. Ion Processes*, **1996**, *135*, 173, and references therein.

(38) Calculated values according to eqs 1a–1e, experimental ratios in parentheses: H<sub>2</sub>/HD (**17a**/Fe<sup>+</sup>) = 0.50 (0.48); H<sub>2</sub>/HD (**17b**/Fe<sup>+</sup>) = 0.04 (0.05); H<sub>2</sub>/HD (**17c**/Fe<sup>+</sup>) = 2.08 (1.96); H<sub>2</sub>/HD (**17d**/Fe<sup>+</sup>) = 8.00 (7.73); H<sub>2</sub>/HD (**17e**/Fe<sup>+</sup>) = 98.0 (65.0). Considering the experimental uncertainty and the limitations of the applied model, the agreement is quite satisfactory and demonstrates the validity of the approach.

(36) (a) Lebrilla, C. B.; Drewello, T.; Schwarz, H. *Int. J. Mass Spectrom. Ion Processes* **1987**, *79*, 287. (b) Drewello, T.; Eckart, K.; Lebrilla, C. B.; Schwarz, H. *Int. J. Mass Spectrom. Ion Processes* **1987**, *76*, R1. (c) Stepnowski, R. M.; Allison, J. *Organometallics* **1988**, *7*, 2097. (d) Lebrilla, C. B.; Drewello, T.; Eller, K.; Zummack, W.; Schwarz, H. *Int. J. Mass Spectrom. Ion Processes* **1990**, *100*, 803.

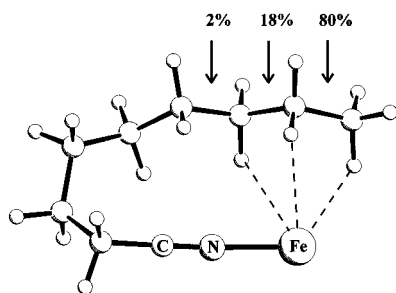


**Figure 2.** Experimentally determined regioselectivities for the unimolecular dehydrogenation of metastable nonanitrile/ $\text{Fe}^+$ . The experimental data were obtained using eqs 1a–1e.

with the parameters  $k_{\text{C}(8)/\text{C}(9)} = 0.80$ ,  $k_{\text{C}(7)/\text{C}(8)} = 0.18$ , and  $k_{\text{C}(6)/\text{C}(7)} = 0.02$ . Note that the magnitude of the KIE is in accord with the data of **17c**/ $\text{Fe}^+$  and with previous studies of nitrile/ $\text{Fe}^+$  complexes.<sup>39</sup> Due to this internal consistency of the solution for eqs 1a–1e, the relative rate constants  $k_i$  can be regarded as reasonable representatives for the regioselectivities of C–H bond activation in the various positions of the nitrile (Figure 2).

The experimentally determined regioselectivities show pleasing agreement with the computational predictions in which the calculated activation barriers follow the same order. Note, however, that the experiment cannot discriminate between the variants of endo- and exocyclic pathways.

The generation of methane is a minor reaction channel for nonanitrile/ $\text{Fe}^+$  with an intensity of only 2% of all neutral products formed. Nevertheless, the reaction is highly regioselective, since **17a**/ $\text{Fe}^+$  eliminates only  $\text{CD}_3\text{H}$  ( $\Delta m = 19$ ), **17d**/ $\text{Fe}^+$  exclusively loses  $\text{CH}_3\text{D}$  ( $\Delta m = 17$ ), and all other complexes give rise to  $\text{CH}_4$  ( $\Delta m = 16$ ). Thus, unimolecular formation of methane can conveniently be described in terms of a 1,2-elimination process as described in previous experimental investigations.<sup>2,4,36</sup> In view of the theoretical predictions, the reactions proceed via initial insertion of  $\text{Fe}^+$  into the terminal C–C bond, followed by  $\beta$ -hydrogen transfer and loss of methane, rather than involving C–H bond activation as the first step and subsequent  $\beta$ -methyl migration.<sup>40,41</sup>

The generation of neutral olefins, i.e., ethene ( $\Delta m = 28$ ), propene ( $\Delta m = 42$ ), and butene ( $\Delta m = 56$ ), represents the third reaction pathway of the metastable  $\text{Fe}^+$  complexes of isotopologous nonanitriles. These reactions proceed cleanly without involving any H/D exchange processes. Because theory predicts C–C bond insertion as the initial step, the experimentally observed isotope patterns directly reflect the sites for C–C bond activations. The relative intensities of the neutral alkenes formed decrease with increasing size of the neutrals, a behavior that has been described repeatedly in remote functionalization.<sup>4</sup> However, a related study of  $\text{Fe}^+$  complexes of medium-sized aliphatic carbonic

acids has indicated that besides purely energetic aspects, dynamic parameters such as lifetime effects also play a role in these processes.<sup>42</sup> Therefore, the experimentally measured intensities do not necessarily directly correlate with the calculated activation barriers. These predict that loss of ethene should be most difficult among the olefins, while this particular C–C bond activation pathway predominates in the experiment. Due to these uncertainties and the perhaps imperfect choice of model TS **15** (see above), the accuracy of the computational predictions cannot be assessed quantitatively. Nevertheless, qualitative agreement is found because the C–H and C–C bond activation processes can compete with each other as predicted by theory and fully confirmed in the experiment.

**b. Nonanitrile/ $\text{Co}^+$ .** The gas-phase chemistry of “naked”  $\text{Co}^+$  ions with nonanitriles is deceptively similar to the gas-phase reactivity of  $\text{Fe}^+$ . Four classes of neutral products are generated (Table 2), corresponding to the formation of hydrogen, methane, small alkenes, and higher alkanes such as ethane, propane, and butane. Notwithstanding these similarities, distinctly different features with respect to the chemoselectivity, the regioselectivity of the dehydrogenation, and the formation of methane are observed. Furthermore the generation of neutral alkanes, except for methane, is not observed at all in the metastable ion spectra of the analogous  $\text{Fe}^+$  complexes and represents a unique feature of the  $\text{Co}^+$  complexes. The similarities and differences between the reactivities of  $\text{Fe}^+$  and  $\text{Co}^+$  will be discussed in the following section.

The first apparent difference concerns the different chemoselectivity for the  $\text{Co}^+$  complexes. Though dehydrogenation still dominates for **17**/ $\text{Co}^+$ , it is much less intense (39% of all products) as compared to the  $\text{Fe}^+$  analog. As a consequence, C–C bond activation processes play a larger role. Further, the distribution of olefins formed is somewhat smoother for nonanitrile/ $\text{Co}^+$  in that the formation of the higher olefins propene and butene is much more pronounced than in the  $\text{Fe}^+$  system.

As far as the generation of neutral hydrogen from the  $\text{Co}^+$  complexes of nonanitrile is concerned, we can again deconvolute the data according to eqs 1a–1e. This procedure results in an averaged primary kinetic isotope effect of  $k_{\text{H}_2}/k_{\text{HD}} = 1.5$  and the regioselectivities depicted in Figure 3. However, the solution is less internally consistent, thus pointing toward the operation of a more complex kinetic scheme. Most likely, this complication arises from isotopically sensitive branching<sup>37</sup> among the different dehydrogenation pathways: For example, the  $\text{H}_2/\text{HD}$  ratio for **17c**/ $\text{Co}^+$  indicates a KIE of  $\sim 1.5$ . Taking this value for the deconvolution of the data of **17b**/ $\text{Co}^+$ , one is forced to assume that at least 10% of the hydrogen formed stems from internal positions <C(7); however, this result is clearly in contradiction with the small amount of HD formed from **17e**/ $\text{Co}^+$ . Despite these uncertainties, it is nevertheless obvious from the experimental data that the KIE as well as the selectivity for activation at C(9) are lower in the  $\text{Co}^+$  complexes as compared to the  $\text{Fe}^+$  species.

The generation of neutral methane from the  $\text{Co}^+$  complexes of nonanitrile is in terms of the mechanistic

(39) (a) Czekay, G.; Drewello, T.; Eller, K.; Zummack, W.; Schwarz, H. *Organometallics* **1989**, *8*, 2439. (b) Czekay, G.; Drewello, T.; Schwarz, H. *J. Am. Chem. Soc.* **1989**, *111*, 4561. (c) Czekay, G.; Eller, K.; Schröder, D.; Schwarz, H. *Angew. Chem., Int. Ed. Engl.* **1989**, *28*, 1277.

(40) See, for example: Watson, P. L.; Roe, D. C. *J. Am. Chem. Soc.* **1982**, *104*, 6471.

(41) For an unambiguous example of  $\beta$ - $\text{CH}_3$  migration and further references, see: Karrass, S.; Schwarz, H. *Organometallics* **1990**, *9*, 2409.

(42) Schröder, D.; Zummack, W.; Schwarz, H. *J. Am. Chem. Soc.* **1994**, *116*, 5857.

**Table 2. Mass Differences (amu) Observed in the Unimolecular Fragmentations of Isotopologous Co<sup>+</sup> Complexes of 17–19<sup>a,b</sup>**

precursor	$\Delta m$																						
	2	3	16	17	18	19	28	29	30	31	32	33	42	43	44	45	46	47	56	57	58	59	61
<b>17</b>	39		6				26		8				15		2			4					
<b>17a</b>	18	22	1	2		3			21		8					17		2				6	
<b>17b</b>	5	27	3	3					27		9			16	1		3			1	5		
<b>17c</b>	20	12	6	2				26		11			5	10		3				5			
<b>17d</b>	31	9	1	2	3		25		9	1					13		3			3			
<b>17e</b>	45	2	5	1			25		2	3			12		2						3		
<b>18</b>	32		10				20		13				18		3				3		1		
<b>18a</b>	22	10	2	2		5			15			13		1	21		4					4	1
<b>19</b>	25		11				14		10				25		6				8		1		
<b>19a</b>	20	6	3	2		6			10			10		2	26		6					8	1

<sup>a</sup> Intensities are normalized to  $\sum_{\text{reactions}} = 100\%$ . <sup>b</sup> Reactions with intensities of <1% are omitted.

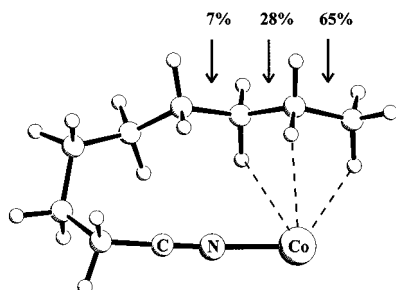


**Figure 3.** Experimentally determined regioselectivities for the unimolecular dehydrogenation of metastable nonanitrile/Co<sup>+</sup>. The experimental data were deconvoluted using eqs 1a–1e.

scenario strikingly different from the one of the corresponding Fe<sup>+</sup> complexes. The isotope distribution in the neutral products observed in the metastable ion spectra of the Co<sup>+</sup> complexes of the isotopologs **17a**–**17e** can only be rationalized if one assumes that the carbon atoms C(7) and C(9) equilibrate prior to loss of methane. Similar degenerate rearrangements of the carbon skeleton have previously been proposed to occur in nitrile/M<sup>+</sup> complexes.<sup>43</sup> However, it is not the scope of this paper to discuss the peculiar mechanistic details of a minor reaction channel with only 6% intensity of all products formed, and we refrain from suggesting a speculative model to account for this process.

The most significant difference in the gas-phase reactivity of Co<sup>+</sup> versus Fe<sup>+</sup> with linear aliphatic nitriles is the generation of neutral alkanes such as ethane, propane, and butane as observed in the reaction of the Co<sup>+</sup> complexes. These reactions can be rationalized similar to the loss of methane via an initial C–C bond activation, followed by an endocyclic  $\beta$ -H transfer, and a final elimination of the neutral. Though consecutive losses of an olefin and a hydrogen molecule have been reported to occur in remote functionalization,<sup>39,44</sup> this conjecture can be ruled out in the present case, based on MS<sup>3</sup> experiments<sup>45</sup> which demonstrate that for **17**/Co<sup>+</sup> no consecutive losses of H<sub>2</sub> and an olefin is operative; hence, the alkanes are expelled as intact units.

**c. Deca- and Undecanitrile/M<sup>+</sup>.** A crucial aspect with respect to the more general relevance of the

computational study concerns the question of whether the preferential C–H bond activation at C(8)/C(9) represents an intrinsic feature in remote functionalization or whether this preference is confined to nonanitrile. Therefore, we also examined the M<sup>+</sup> complexes of the larger C<sub>10</sub> and C<sub>11</sub> nitriles **18** and **19** as well as their [ $\omega, \omega, \omega$ -D<sub>3</sub>]-isotopologs.

At first, the existence of remote functionalization is further confirmed by the reactions of these complexes, because the types of unimolecular processes observed coincide with those of nonanitrile/M<sup>+</sup>. In general, upon further elongation of the chain, the C–C bond activation processes increase in intensity at the expense of dehydrogenation of **18**/M<sup>+</sup> and **19**/M<sup>+</sup>. Assuming the same type of analysis as we have used above and adopting also the kinetic isotope effect for the Fe<sup>+</sup> system, we can derive the selectivities for C–H bond activation of the terminal positions. Thus, it can be estimated for **18a**/Fe<sup>+</sup> and **19a**/Fe<sup>+</sup> that 50 and 40%, respectively, of the dehydrogenation occurs from the  $\omega/(\omega - 1)$  positions. As compared to a selectivity as large as 80% for C–H bond activation at C(8)/C(9) in nonanitrile/Fe<sup>+</sup>, the experimental data clearly demonstrate that with increasing chain length the activation of terminal methyl group of linear nitriles by Fe<sup>+</sup> ions becomes less favorable, whereas the activation of internal positions competes more effectively. Thus, the experiments reveal that these particular C–H bonds are the preferential positions for bond activation in nitriles and that this site selectivity is a fundamental property of the whole series of RCN/Fe<sup>+</sup> rather than just a remnant of the particular system studied. This finding unambiguously proves that there is an energetically and geometrically favored position for C–H bond activation by Fe<sup>+</sup> ions in the gas phase. Thus, the results perfectly justify the choice of the model system which we examined in the theoretical part; note, however, that this choice was made before any experiments were performed in this direction and it was simply based on plausibility considerations as well as the limitations in the computational treatment.

A very similar situation is found for the Co<sup>+</sup> complexes of **18** and **19**. As discussed for nonanitrile/M<sup>+</sup>, the comparison shows that the selectivity for C–H bond activation is in general smaller for Co<sup>+</sup>. Further, application of the same type of analysis to **18a**/Co<sup>+</sup> and **19a**/Co<sup>+</sup> results in regioselectivities of about 45 and 35%, respectively, for the dehydrogenation of the terminal positions.

### C. Comparison of Theoretical Predictions with

(43) Eller, K.; Zummack, W.; Schwarz, H.; Roth, L. M.; Freiser, B. S. *J. Am. Chem. Soc.* **1991**, *113*, 833.

(44) Schröder, D.; Schwarz, H. *J. Am. Chem. Soc.* **1990**, *112*, 5947.

(45) The H<sub>2</sub> elimination product of the Co<sup>+</sup>/nonanitrile complex has been mass selected by means of B1 and E1, and the metastable ion decomposition spectra have been recorded with the subsequent magnetic sector B2. No olefin loss is observed, thus ruling out a consecutive reaction mechanism.

**Table 3. Experimentally Determined Regioselectivities for Unimolecular Dehydrogenation of Nonanitrile/M<sup>+</sup> and Calculated Barrier Heights for C–H Bond Activation of the Respective Positions**

	positions	selectivity (%) <sup>a</sup>	calcd barriers (kcal mol <sup>-1</sup> )
nonanitrile/Fe <sup>+</sup>	C(6)/C(7)	2 (3)	34 <sup>b</sup> ( <i>exo</i> )/38 ( <i>endo</i> )
	C(7)/C(8)	18 (17)	29 ( <i>exo</i> )/34 ( <i>endo</i> )
	C(8)/C(9)	80 (80)	24 ( <i>exo</i> )/33 ( <i>endo</i> )
nonanitrile/Co <sup>+</sup>	C(6)/C(7)	7 (10)	37 <sup>b</sup> ( <i>exo</i> )/42 ( <i>endo</i> )
	C(7)/C(8)	28 (25)	32 ( <i>exo</i> )/38 ( <i>endo</i> )
	C(8)/C(9)	65 (65)	26 ( <i>exo</i> )/36 ( <i>endo</i> )

<sup>a</sup> Predicted selectivities in parentheses using the Arrhenius formalism and assuming an effective temperature of 1550 K for nonanitrile/Fe<sup>+</sup> and 2900 K for nonanitrile/Co<sup>+</sup>, respectively; see text and ref 46. <sup>b</sup> Estimated barrier; see text.

**the Experimental Findings.** Prior to a comparison of the theoretical predictions with the experimental data, it is worth pointing out that the experimental study cannot assess whether dehydrogenation occurs in an endo- or exocyclic manner. Therefore, only the overall selectivities for dehydrogenation of nonanitrile/M<sup>+</sup> from the positions C(6)/C(7), C(7)/C(8), and C(8)/C(9), respectively, can be compared with theory; note that the entry for C(6)/C(7) represents all C–H bond activations of internal positions. Further, the computations do not cover the probably favored exocyclic elimination involving C(6)/C(7). In view of the fact that the experiment shows that this particular pathway is indeed of minor importance, we refrained from an explicit calculation of the corresponding insertion structure as well as the related model TS. Instead, we assume that the difference between TS **6** and TS **10** translates to the TS associated with exocyclic elimination of hydrogen from C(6)/C(7) and estimate the height of the barrier as 34 kcal mol<sup>-1</sup> relative to the minimum **2**.

The comparison of the calculated barrier heights with the measured selectivities reveal a pleasing agreement (Table 3). In fact, the experimentally measured regioselectivities can nicely be reproduced in a simplified formalism, assuming an Arrhenius-type behavior according to the eqs 2a–2c for an internal ion temperature

$$k_{C(8)/C(9)} \propto \exp(-24 \text{ kcal mol}^{-1}/RT) + 1.5 \exp(-33 \text{ kcal mol}^{-1}/RT) \quad (2a)$$

$$k_{C(7)/C(8)} \propto \exp(-29 \text{ kcal mol}^{-1}/RT) + \exp(-34 \text{ kcal mol}^{-1}/RT) \quad (2b)$$

$$k_{C(6)/C(7)} \propto \exp(-34 \text{ kcal mol}^{-1}/RT) + \exp(-38 \text{ kcal mol}^{-1}/RT) \quad (2c)$$

of ~1550 K for nonanitrile/Fe<sup>+</sup>. Here, the activation barriers are those of TS **6**–TS **10**, respectively.

The preexponential factors for the different reactions are assumed to be identical; the factor of 1.5 in the relation for  $k_{C(8)/C(9)}$  corrects for the higher statistical propensity for C–H bond activation of the terminal methyl group. Subsequently, the effective temperature  $T$  has been fitted in order to reproduce the experimentally measured selectivities.<sup>46</sup> Thus, C–H bond activa-

tion at the terminus is clearly preferred, in terms of both the lowest activation barrier calculated for TS **6** and the experimental finding. Following the energetic order of the model TSs, C–H bond activation across C(7)/C(8) can compete with this process, but is less abundant; dehydrogenation of internal positions is almost negligible.

In general, the agreement for the Co<sup>+</sup> system is also satisfactory, but the deviations are somewhat larger, most probably due to the isotopically sensitive branching that is operative in this system and that deteriorates the evaluation of the experimental regioselectivities (see above). Most notable is, however, the significantly higher effective temperature (2500–3000 K)<sup>47</sup> necessary to model dehydrogenation of the various sites for the cobalt complexes. As compared to the Fe<sup>+</sup> complexes, a higher effective temperature of the Co<sup>+</sup> complexes is not only consistent with higher activation barriers for this metal but also accounts for the decrease of the KIE and the lower selectivity as far as C–H and C–C bond activation by Co<sup>+</sup> is concerned.

As a major result of this analysis, we can conclude that the lower selectivity in the Co<sup>+</sup> system in comparison to Fe<sup>+</sup> is not due to different reaction trajectories for the two metals but rather simply a result of the increased internal energy. Thus, the previous interpretation of experimental results for nitrile/M<sup>+</sup> complexes needs to be revised in that the directionalities for remote bond functionalization by Fe<sup>+</sup> and Co<sup>+</sup> are virtually identical, and it is rather the difference in internal energy that leads to the preferential insertion of Co<sup>+</sup> into more internal C–H or C–C bonds.

**D. Implications for the General Concept of Remote Functionalization.** The results of this combined theoretical and experimental effort study have several consequences with respect to the interpretation of previous experiments.

(i) The different chain length dependencies reported previously to be operative in remote functionalization by Fe<sup>+</sup> and Co<sup>+</sup>, respectively, do not necessarily reflect intrinsic features of the reaction trajectories for these two metals. Rather, the lower selectivity of Co<sup>+</sup> as compared to Fe<sup>+</sup> seems to be a consequence of the larger activation barriers for Co<sup>+</sup>. Thus, in conjunction with the higher BDEs of Co<sup>+</sup> to organic ligands, the internal energy of the resulting complexes is larger than in the Fe<sup>+</sup> case, such that selectivities decrease. Therefore, the interpretation of chain length dependencies with respect to the preferential sites for C–H and C–C bond activations by different metal cations<sup>6,34</sup> or different modes of coordination to the functional group<sup>48</sup> must carefully account for internal energy effects. Further, the slight deviations of experiment and theory as far as the olefin losses are concerned support the previous suggestion that for metastable ions of a size like nonanitrile/M<sup>+</sup> dynamic parameters play a significant

(47) Note that these effective temperatures are not in contradiction with those used in the estimation of the BDE using the kinetic method. This conclusion simply considers that the rearrangements giving rise to remote functionalization are associated with sizeable activation barriers such that the internal energies of the metastable ions can be significant. In contrast, loss of a ligand from bisligand complexes of the type M(L)(L')<sup>+</sup> occurs as a continuously endothermic process without any significant barrier such that the internal energy that can be stored in these ions is much smaller, given that a similar time scale for unimolecular dissociation is sampled in both experiments.

(48) Chen, L.-Z.; Miller, J. M. *Can. J. Chem.* **1991**, *69*, 2002.

(49) Schröder, D.; Schwarz, H. *J. Am. Chem. Soc.* **1993**, *115*, 8818.

(46) Note that this formalism is hardly affected by the absolute heights of the barriers and only depends upon the difference for the various positions.

role such that arguments solely relying on minima and TSs are not sufficient for a concise description of the relative intensities of the fragments formed.

(ii) The multicentered nature of the TSs for the unimolecular dehydrogenation enforces a reinterpretation of the previous assignments of the reductive elimination of dihydrogen from a suggested dihydrido intermediate as the rate-determining step in remote functionalization. These assignments were based on a careful analysis of kinetic isotope effects associated with dehydrogenation of different labeled complexes, for which it was found that the positioning of the label hardly effects the KIE which, hence, is only due to the formation of H–H, H–D, and D–D bonds, respectively. In view of the theoretical finding that these suggested dihydrido species are nonexistent for late transition-metal cations, the experimental KIEs are consistent with the concerted nature of the multicentered TSs.

(iii) Finally, the present study demonstrates in which way even small differences in activation barriers can affect branching ratios of competing channels in metastable ion decomposition. This result is in perfect agreement with the observation of diastereoselective discriminations in the remote functionalization of a variety of flexible substrates as different as nitriles,<sup>9</sup> ketones,<sup>49</sup> and carboxylic acids<sup>42</sup> by bare Fe<sup>+</sup> and Co<sup>+</sup>. Moreover, with regard to the high effective temperatures of the metastable nitrile/M<sup>+</sup> complexes, the diastereoselectivities determined so far propose that the intrinsic stereoselectivity in remote functionalization is large, rendering it a promising candidate for highly selective bond activation processes under more thermal conditions.

### Conclusions

The experimental confirmation of the theoretical predictions for the nonanitrile/M<sup>+</sup> system by the experimentally measured regioselectivities represents a rather impressive demonstration of the performance of nowadays theoretical methods. This success was possible only by a combination of modern quantum chemical methods with empirical force field calculations in order to allow for a proper description of the organometallic part as well as consideration of the conformational space. The experimental data for the nitriles **17–19** reveal that nonanitrile/M<sup>+</sup> can serve as a useful representative as far as regioselectivity of dehydrogenation

is concerned and by such confirm the choice of the model system in the calculations. Nevertheless, the combination of quantum chemistry and molecular mechanics goes in hand with several disadvantages; namely, the saddle point searches are always restricted to the construction of model transition structures, and further, vibrational frequencies and thus zero-point energy and thermal corrections cannot be assessed. The latter aspect is particularly unfortunate because several findings in this study indicate that dynamic treatment of the nonanitrile/M<sup>+</sup> system is indicated and entropy factors do certainly influence chemo- and regioselectivities.

With respect to remote functionalization in the gas phase, the present analysis of the unimolecular dehydrogenation of nonanitrile/M<sup>+</sup> demonstrates that the essence of the concept is rather simple, i.e., precomplexation of the metal to a dative ligand which then provides chemo-, regio- and, as shown in a different context,<sup>9,49</sup> stereoselectivity. Moreover, the preferential trajectory for C–H bond activation around C(9) of the aliphatic chain resembles the enzymatic dehydrogenation of saturated fatty acids with regard to the particular site selectivity. While in biological systems the selectivity is certainly determined by the ligand environment of the reactive non-heme iron center,<sup>50</sup> the preference observed here points toward an intrinsically favored trajectory for bond activation in this region of the chain. In particular, the latter finding is a promising conjecture and challenges the chemical community to search for analogs to this type of remote functionalization in the condensed phase.

**Acknowledgment.** Financial support by the Deutsche Forschungsgemeinschaft, the Volkswagen-Stiftung, and the Fonds der Chemischen Industrie is acknowledged. M.C.H. gratefully acknowledges financial support from the Gesellschaft von Freunden der Technischen Universität Berlin. Computer time on the CRAY J90 system and excellent service (Dr. T. Steinke) was provided by the Konrad-Zuse Zentrum für Informationstechnik, Berlin. Finally, we thank Drs. Andreas Fiedler and Jeremy N. Harvey for helpful discussions.

OM970229W

(50) (a) Kaim, W.; Schwederski, B. *Bioorganische Chemie*; Teubner: Stuttgart, 1991. (b) Lippard, S. J.; Berg, J. M. *Principles of Bioinorganic Chemistry*; University Science Books: Hill Valley, CA, 1984.